Atypical chemokine receptor 1 on nucleated erythroid cells regulates hematopoiesis

Published in final edited form as:
Nat Immunol. 2017 July ; 18(7): 753–761. doi:10.1038/ni.3763.

Atypical chemokine receptor 1 on nucleated erythroid cells regulates hematopoiesis

Johan Duchene[1,14], **Igor Novitzky-Basso**[2,14], **Aude Thiriot**[3,4,15], **Maria Casanova-Acebes**[5,15], **Mariaelvy Bianchini**[1,15], **S. Leah Etheridge**[6,15], **Elin Hub**[6], **Katrin Nitz**[1,7], **Katharina Artinger**[6,8], **Kathrin Eller**[8], **Jorge Caamaño**[9], **Thomas Rülicke**[10], **Paul Moss**[9], **Remco T. A. Megens**[1,11], **Ulrich H. von Andrian**[3,4], **Andres Hidalgo**[1,5], **Christian Weber**[1,11,16], and **Antal Rot**[1,6,12,13,16]

[1]Institute for Cardiovascular Prevention, Ludwig-Maximilians-University, Munich, Germany [2]Blood and Marrow Transplant Unit, Queen Elizabeth University Hospital, Glasgow UK [3]Department of Microbiology and Immunobiology and Center for Immune Imaging, Harvard Medical School, Boston, MA, USA [4]The Ragon Institute, Cambridge, MA, USA [5]Fundación Centro Nacional de Investigaciones Cardiovasculares Carlos III, Madrid, Spain [6]Centre for Immunology and Infection, Department of Biology, University of York, Heslington, York, UK [7]Max Delbrück Center for Molecular Medicine in the Helmholtz Association, Berlin, Germany [8]Clinical Division of Nephrology, Department of Internal Medicine, Medical University of Graz, Graz, Austria [9]Institute of Immunology and Immunotherapy, College of Medical and Dental Sciences, University of Birmingham, Birmingham, UK [10]Institute of Laboratory Animal Science, University of Veterinary Medicine Vienna, Vienna, Austria [11]Cardiovascular Research Institute Maastricht, University of Maastricht, Maastricht, The Netherlands [12]Center for Advanced Studies, Ludwig-Maximilians-University, Munich, Germany [13]Address from July 2017: William Harvey Research Institute, Queen Mary University of London. London, UK

Abstract

Healthy individuals of African ancestry have neutropenia that has been linked with the variant rs2814778(G) of the gene encoding atypical chemokine receptor 1 (ACKR1). This polymorphism selectively abolishes the erythroid cell expression of ACKR1, causing Duffy-negative phenotype. Here we describe an unexpected fundamental role that ACKR1 plays in hematopoiesis and provide the mechanism linking its absence with neutropenia. Nucleated erythroid cells highly expressed

[16]Correspondence should be addressed to A.R. (a.rot@qmul.ac.uk) or C.W. (chweber@med.lmu.de).
[14]First authors, equal contribution;
[15]Equal contribution;

Accession codes

The complete microarray dataset is deposited in the Gene Expression Omnibus (GEO) database (http://www.ncbi.nlm.nih.gov/geo) under accession no. GSE86349.

Authors contributions

A.R. conceived the study; J.D., I.N-B., R.T.A.M., U.H.v.A., A.H., C.W. and A.R. designed the experiments; J.D., I.N-B, A.T., M.C-A, M.B., S.L.E., E.H., K.N., K.A. and T.R. performed the experiments and evaluated the data; J.D., I.N-B., K.E., J.C., P. M., R.T.A.M., U.H.v.A., A.H., C.W. and A.R. interpreted the data; A.R, J.D. and C.W. wrote the manuscript.

The authors declare no conflict of interest.

Europe PMC Funders Author Manuscripts

ACKR1, which facilitated their direct contacts with the hematopoietic stem cells. The absence of erythroid ACKR1 altered murine hematopoiesis, including stem and progenitor cells, ultimately giving rise to phenotypically distinct neutrophils, which readily left the circulation, causing neutropenia. Duffy-negative individuals developed a distinct profile of neutrophil effector molecules closely reflecting that in the ACKR1-deficient mice. Thus, alternative physiological patterns of hematopoiesis and bone marrow cell outputs depend on the expression of ACKR1 in the erythroid lineage providing major implications for the selection advantages that have resulted in the paramount fixation of the rs2814778(G) polymorphism in Africa.

Introduction

Chemokines comprise a family of structurally homologous, intercellular molecular signals that induce migration and other cellular responses, including adhesion, activation, differentiation, proliferation and survival1–4. Chemokine effects are mediated by classical G-protein coupled receptors (GPCRs)1,2. Additionally, chemokines ligate atypical chemokine receptors (ACKRs)5,6. ACKRs are structurally similar to GPCRs but do not couple to G-proteins and therefore fail to induce the full spectrum of downstream intracellular signals that characterize GPCRs7,8. However ACKRs may transport, present or scavenge chemokines and thus, by different means, effectively regulate chemokine availability in tissue microenvironments9–12. The atypical chemokine receptor 1 (ACKR1), previously known as Duffy antigen receptor for chemokines or DARC, binds over 20 different CC and CXC chemokines13,14 and has been ascribed a unique profile of cell expression in cerebellar neurons, venular endothelial cells and erythrocytes13,14. ACKR1 in endothelial cells transports and presents chemokines9. ACKR1 on erythrocytes was shown to regulate chemokine concentrations in plasma, acting as both chemokine sink and reservoir15–17 and to bind *Plasmodium (P.) vivax* and *P. knowlesi,* thus allowing their erythrocyte invasion18,19.

Divergent paths of human evolution and adaptations to geographically restricted microbial pathogens resulted in the development of distinctive functions of the immune system that characterize people of different ethnicities20,21. Under physiological conditions, individuals of African ancestry have low blood neutrophil counts22. Such “ethnic neutropenia” has been directly linked with the allelic variant rs2814778(G) of *ACKR1* that is hugely prevalent in Africa, but the mechanism behind this association remained unexplored23. Individuals of African ancestry who are homozygous for the rs2814778(G) allele do not express ACKR1 on erythrocytes24,25. This “Duffy-negative” phenotype is caused by one nucleotide substitution within the promoter of *ACKR1,* which disrupts the sequence binding the erythroid transcription factor GATA-1 and leads to the selective loss of ACKR1 expression in erythrocytes but not endothelium26,27. Erythrocytes are terminally differentiated anuclear cells with no transcription and limited translation28, suggesting that the expression of ACKR1 might occur first during the earlier stages of erythroid cell development in the bone marrow (BM). We therefore sought to determine ACKR1 expression in the BM, to investigate its impact on hematopoiesis and explore the mechanism leading to neutropenia in the absence of erythroid ACKR1.

Results

ACKR1 is highly expressed by nucleated erythroid cells

We used a new specific monoclonal anti-mouse ACKR1 antibody29 to map ACKR1 expression in mouse BM. Apart from the endothelial cells (ECs), which line BM sinusoids, ACKR1 expression was detected only on erythroid cells but not on any other hematopoietic population (Fig. 1a–c and Supplementary Fig.1 and Supplementary Fig.2). Nucleated erythroid cells (NECs) expressed ACKR1, initially in proerythroblasts, peaking in early normoblasts and gradually declining to the lowest expression in mature erythrocytes (Fig. 1c and Supplementary Fig. 2b). ACKR1 on NECs was functional. Fluorescently-labeled CCL2, an ACKR1-cognate chemokine, bound to NEC subpopulations proportionately to the levels of their ACKR1 expression (Fig.1d). Even after extended pre-incubation, almost all NEC-bound CCL2 could be removed from binding by a heterologous chemokine CXCL1 (Fig. 1d). ACKR1 is the only chemokine receptor, which binds both CCL2 and CXCL1. Thus, ACKR1 on NECs did not actively scavenge chemokines, which remained available on the cell surface. In summary, our data unequivocally showed that, among hematopoietic BM cells, ACKR1 is expressed in the erythroid lineage only. The high level of ACKR1 expression and chemokine binding by NECs, as compared to mature erythrocytes, suggested that ACKR1 might play an important physiological role in the BM.

ACKR1 deficiency alters early hematopoiesis

To evaluate the contribution of ACKR1 expression to BM homeostasis, we compared parameters of hematopoiesis in ACKR1-deficient30 and wild-type mice. ACKR1 expression had no effect on the overall BM cellularity, number of erythroid cells, relative proportions of their individual subpopulations or any of the erythrocyte parameters in blood (Supplementary Fig. 3). However, ACKR1 expression had cell-extrinsic effects on the BM hematopoietic stem and progenitor cells (HSPCs). In the absence of ACKR1, the size of the lineage-negative (Lin^-) $Sca\text{-}1^+$ $c\text{-}Kit^+$ cell (LSK) population decreased (Fig. 2a), accompanied by their reduced proliferation (Fig. 2b) and increased surface expression of CD34 (Fig. 2c). Major reduction was seen in the $CD48^-$ subpopulation of LSKs (Fig. 2d and Supplementary Fig. 4a). Furthermore, we observed shifts in the proportions of individual LSK $CD48^-$ subpopulations of ACKR1-deficient mice, as compared to their wild-type littermates (Fig. 2e,f). These included an increased relative proportion of hematopoietic stem cells (HSCs; Fig. 2e), although their overall numbers remained unaltered (Fig. 2f), as well as a relative and an absolute decrease of the $CD150^-$ $Flt3^-$ and $CD150^-Flt3^+$ multipotent progenitor cells (MPP) 1a and 1b (Fig. 2e,f). Furthermore, the size of the $Lin^-Sca\text{-}1^-c\text{-}Kit^+$ myeloid progenitor cell (MPC) population was reduced in ACKR1-deficient BM (Fig. 2g), due to decrease in populations of $CD34^+$ $CD16/32^+$ granulocytic-monocytic progenitor (GMP) and $CD34^-$ $CD16/32^-$ megakaryocytic-erythroid progenitor (MEP) cells (Fig. 2h,i). Conversely, the proportions of $CD34^+$ $CD16/32^-$ common myeloid progenitor (CMP) cells and LSK $CD48^+Flt3^-$ (MMP2) cells increased in the ACKR1-deficient BM (Fig. 2h,i and Supplementary Fig. 4b-d), whereas the numbers of LSK $CD48^+$ cells, lineage-restricted progenitor (LRP) cells and common lymphoid progenitor (CLP) cells remained unchanged (Supplementary Fig. 4b,d,e). Thus the absence of ACKR1 resulted in numeric changes and

shifts in equilibria of HSPC subpopulations and led to characteristic changes in the expression of their surface effector molecules.

ACKR1 deficiency changes HSPC transcriptome

Next, we asked whether ACKR1 expression also affected the transcriptional makeup of HSPCs. To this end, LSK and GMP cells of ACKR1-deficient and wild-type littermates were sorted by flow cytometry to virtual purity and their transcriptomes were compared using a gene expression microarray. The transcripts for the overwhelming majority of genes were indistinguishable in corresponding cell populations of ACKR1-deficient and wild-type mice (Supplementary Fig. 5a,b). Significant differences primarily included the upregulation of the same set of genes in both LSK and GMP cells of ACKR1-deficient mice (Fig. 3a and Supplementary Fig. 5c), with the majority of these transcripts ascribed as neutrophil- or myeloid-specific (Fig. 3b and Supplementary Fig. 5d). Some of the transcripts of neutrophil-specific effector molecules, including those encoding cathelicidin, neutrophil granule protein and resistin-like molecule-γ, increased in GMPs from ACKR1-deficient BM a thousand-fold or more (Supplementary Fig. 5b), although upregulated genes represented only a part of the characteristic neutrophil transcriptome and excluded some classical neutrophil markers (Fig. 3c). Thus, the absence of ACKR1 lead to an upregulation of a subset of neutrophil and other mature cell-specific transcripts in HSPCs, findings consistent with altered differentiation of HSPCs. Together with the observed numeric and surface molecule changes in HSPC subsets, these data indicated that ACKR1 expression massively impacted on the balanced BM homeostasis of HSPCs.

ACKR1 on bone marrow NECs affects HSPCs

In the BM ACKR1 is expressed by sinusoidal ECs and NECs. Vessels in the BM serve as a HSPC niche[31–33], whereas NECs have not previously been shown to impact on HSPC homeostasis. To explore whether the HSPC changes observed in ACKR1-deficient mice were due to the lack of ACKR1 expression in ECs, NECs or both, HSPC parameters were recorded in reciprocal irradiation BM-chimeric wild-type and ACKR1-deficient mice. Mice in individual groups expressed ACKR1 in either hematopoietic or stromal compartments, or in both or were globally ACKR1-deficient (Supplementary Fig. 6a-c). The characteristic for the ACKR1-deficient mice shifts in the HSPC populations and changes in the expression of CD34 on LSK cells, were associated in chimeric mice, which lacked ACKR1 expression in hematopoietic but not stromal compartments (Fig. 4a-c and Supplementary Fig. 6d). These data clearly pinpointed ACKR1 expressed in erythroid cells as a regulator of HSPC homeostasis.

Next, we asked whether ACKR1 expressed by circulating erythrocytes or by BM NECs might impact on HSPCs. To this end, we created parabiotic wild-type and ACKR1-deficient mice, which shared a common blood circulation but maintained their distinct tissue microenvironments, including those in the BM (Supplementary Fig.6e). ACKR1 on wild-type erythrocytes that are present within the common circulation restored the plasma concentrations of a cognate chemokine CCL2 in the blood sampled from the ACKR1-deficient parabionts (Supplementary Fig.6f), but failed to affect the characteristic overexpression of CD34 and the disbalance of HSPC populations in their BM (Fig. 5a–c and

Supplementary Fig.6g). Collectively, our data on ACKR1 expression in BM together with the findings in reciprocal BM chimeric and parabiotic mice showed that ACKR1 expressed on BM NECs regulated in trans-geometry the homeostasis of HSPCs.

ACKR1 on NECs promotes direct cell interactions with HSCs

NECs are ubiquitous BM cells that might interact directly with the HSCs and thus affect their behavior. Two-photon microscopy of whole-mount BM preparations allowed unequivocal detection of NECs and HSCs (Supplementary Fig. 7a,b) and showed that NECs formed immediate contacts with the majority of HSCs present in the wild-type BM (Fig. 6a). ACKR1 facilitated the establishment of these close cell encounters, as in the ACKR1-deficient BM only a third of all HSCs directly interacted with NECs (Fig. 6b), while their majority localized at a distance (Fig. 6c and Supplementary Fig. 7c). The direct interactions of HSCs and NECs were sufficiently avid to register as cell duplets in flow cytometry, revealing higher proportions of NEC-HSC duplets in wild-type versus ACKR1-deficient BM (Fig. 6d). Flow cytometry showed that MMP1, MPP2 and LRP also formed direct cell contacts with NECs, however only MMP1 and LRP, but not MPP2 required ACKR1 on NECs for their establishment (Supplementary Fig. 7d). These data uncovered the previously not recognized direct interactions of NECs and HSPCs and the unexpected role that ACKR1 plays in their formation. Together with the observed impact of ACKR1 deficiency on HSPCs, our data suggest that NECs are directly involved in regulating the early stages of hematopoiesis and that ACKR1 deficiency in the erythroid lineage might broadly affect the phenotypes of BM-derived cells.

ACKR1 deficiency alters neutrophil phenotype

We used ACKR1-deficient mice to explore how the absence of ACKR1 in the erythroid lineage might affect neutrophils. Neutrophils that developed downstream of the altered HSPCs in the ACKR1-deficient BM, carried a characteristic molecular signature, most notably overexpression of Fcγ-receptors (FcγR; CD16/32), key molecules involved in neutrophil antimicrobial defenses34 and CD45, a molecule that amplifies FcγR function35, but not several other membrane receptors (Fig. 7a and Supplementary Fig. 8a,b). A similar phenotype characterized neutrophils of healthy Duffy-negative individuals homozygous for the rs2814778(G) ACKR1 allele, which in comparison to neutrophils of Duffy-positive individuals also selectively overexpressed FcγRIIIb (CD16) and CD45 (Fig. 7b). Moreover, neutrophils of both ACKR1-deficient mice and Duffy-negative individuals selectively overexpressed CCR2 (Fig. 7c,d and Supplementary Fig. 8c,d), a key inflammatory chemokine receptor that characterizes monocytes, rather than neutrophils1. Thus, HSPCs, altered in the absence of the erythroid ACKR1, gave rise to phenotypically distinct neutrophils, which overexpressed a set of membrane molecules involved in host defenses. The same set of membrane effector molecules was upregulated on neutrophils of Duffy-negative individuals suggesting that the absence of erythroid ACKR1 due to rs2814778(G) allele might change BM homeostasis by the same mechanism as observed in ACKR1-deficient mice.

ACKR1 deficiency on NEC and its expression on EC cause neutropenia

Healthy Duffy-negative individuals of African ancestry have low blood neutrophil counts22. In contrast, ACKR1-deficient mice had normal neutrophil counts in blood (Fig. 8a) and BM (Supplementary Fig. 8e). Thus, the numeric reductions in the LSK subsets and GMPs observed in ACKR1-deficient mice did not directly lead to neutropenia. Also, ACKR1-deficient mice had normal numbers of all other circulating cell types, despite some changes in the BM (Supplementary Fig. 8e–g). Importantly, Duffy-negative individuals homozygous for the rs2814778(G) allele lack ACKR1 on erythroid cells only, but still express ACKR1 on ECs. To explore whether such a pattern of ACKR1 expression might lead to neutropenia, we studied blood neutrophils in reciprocal wild-type and ACKR1-deficient BM chimeric mice. Wild-type mice reconstituted with ACKR1-deficient BM had characteristically altered neutrophils (Supplementary Fig. 8h) and were indeed neutropenic (Fig. 8b). This finding suggests that the expression of ACKR1 in the venular compartment contributes to neutropenia possibly, in line with its established function in ECs9,36, by facilitating neutrophil exit into the tissues. We explored this hypothesis and asked which tissues might clear the phenotypically altered neutrophils that develop in the absence of NEC ACKR1. Parabiotic wild-type and ACKR1-deficient mice allowed us to directly compare in one artificially created organism the homing of neutrophils of wild-type or ACKR1-deficient mice into individual ACKR1-sufficient or deficient tissues. Neutrophils that developed in ACKR1-deficient BM preferentially homed into spleens of the wild-type parabionts, but not other organs tested, which included BM, liver and lungs (Fig. 8c). In mouse spleen ECs of the red pulp sinusoids expressed ACKR1 (Fig. 8d) in direct accord with the expression of ACKR1 in human spleens (Supplementary Fig. 8i), including in Duffy-negative individuals27. It is not clear if altered neutrophils that migrate into spleen persist there and might contribute to the splenic host defenses. Alternatively, the EC ACKR1-dependent migratory step of neutrophils into the spleen might be part or their clearance from circulation, akin to the mechanism described for neutrophil homing into the BM37. Thus, we show that altered neutrophils, which develop in the absence of ACKR1 on NECs leave circulation causing neutropenia, but only when ACKR1 is expressed by venular ECs, a pattern of ACKR1 expression mirrored in individuals of African ancestry homozygous for the rs2814778(G) allele.

Discussion

Hematopoiesis is a robust process controlled by multiple molecular and cellular cues that maintain HSPCs and regulate their differentiation and proliferation for consistent BM cell outputs32,33. Here we show that ACKR1 expressed by NECs, the most ubiquitous BM cells, regulates the homeostasis of HSPCs and modifies downstream hematopoiesis. The absence of ACKR1 led to altered numbers of HSPCs, due, in part, to their decreased proliferation. It also resulted in shifts in proportions of individual HSPC subpopulations, changes in HSPC transcriptomes, and altered expression of their functional surface molecules. The overall BM cellularity was not affected by ACKR1 and the numeric changes in the individual subpopulations of HSPCs appeared incongruent. The number of HSCs, BM's "reserve" population38,39, was not affected. However, the immediate downstream population, MPP1a, was reduced and MPP1b cells were practically absent from the ACKR1-

deficient BM. This was accompanied by an increase in CMPs, a population downstream of MPP1, which might have resulted from accelerated differentiation from MPP1 to CMP. Alternatively, the numerically increased CMPs may have derived from MPP2 populations, which also increased in the ACKR1-deficient BM, suggesting either a potential contribution of alternative progenitor clones present in the BM40 or pathway plasticity of early HSPC differentiation41. It is possible that changes in expression of molecular markers that were used for definition of HSPCs subpopulations contributed to the numeric differences observed in the ACKR1-deficient BM.

Experiments in ACKR1-deficient chimeric and parabiotic mice unequivocally established that HSPCs were affected by ACKR1 on NECs, but not on the ECs or the circulating erythrocytes. Furthermore, the expression of ACKR1 by NECs increased direct cell contacts between HSPC populations and NECs. These data suggest that ACKR1 determines the function of a HSPCs niche associated with NECs, the existence of which has not been recognized previously. Currently it is not clear whether ACKR1 only mediates the interaction of NECs and HSPCs, but another putative NEC molecule signals to HSPCs. Alternatively, ACKR1 might directly signal to HSPCs, e.g. involving tetraspanin CD82, suggested to bind ACKR1 in trans-geometry42. Recently, CD82 on HSCs has been implicated in maintaining their quiescence through interaction with ACKR1, detected spuriously on BM macrophages using a non-validated antibody43. Indeed, high concentration of this antibody stained BM macrophages, albeit equally well in ACKR1-deficient mice. Based on the immunostaining with a specific antibody and a transcriptome analysis, ACKR1 is not expressed on macrophages neither in the BM nor other tissues29. Nevertheless, it is possible that CD82, either in *trans* on HSPCs or through a *cis* interaction in NECs, might contribute to the effects of ACKR1 on HSPCs. Alternatively, the ACKR1-dependent signal to HSPCs involves one or several of over 20 chemokine ligands of ACKR113. We showed that ACKR1 on NECs binds, but does not scavenge, cognate chemokines, thus potentially acts as a BM reservoir and a universal immobilization template for cognate chemokines. Such function might enable the retention of ACKR1 ligands in NEC-rich BM microenvironments thus allowing them to signal via GPCRs to HSPCs and other BM cells. The chemokine presentation template, ACKR1 on NECs, remains constant, but the signals to HSPCs might change depending on the individual chemokines immobilized and their endless potential combinations that characterize different physiological and pathological conditions. Several among ACKR1-cognate chemokines have been shown to affect HSPCs and hematopoiesis44, although CXCL12, which plays a key role in HSPC homeostasis45, does not bind ACKR146.

The absence of ACKR1 caused a shift in HSPC transcriptome, primarily massive overexpression of a subset of neutrophil- and myeloid-specific genes. This is consistent with altered differentiation of HSPCs towards the myeloid lineage and suggests that the characteristic molecular signature of neutrophils observed in ACKR1-deficiency might be imprinted already during the early steps of hematopoiesis. The signature changes in neutrophils that originated in the ACKR1-deficient BM were required, but not sufficient alone, to cause neutropenia. The BM chimeric mice showed that neutropenia developed only when the absence of BM ACKR1 was combined with the expression of ACKR1 in the venular ECs. Mechanistically this is in concert with the known contribution of ACKR1 on

ECs to optimal chemokine-driven neutrophil egress into the tissues9 and explains why globally ACKR1-deficient mice, despite generating altered neutrophils, were not neutropenic. Accordingly, in parabiosis experiments the emigration of the phenotypically altered neutrophils of the ACKR1-deficient parabionts took place preferentially into the spleens of wild-type mice. In addition to the spleen, venular ECs in several other organs and tissues, including the skin and the gut, but not the liver or the lungs, express ACKR129. Thus, neutrophils that develop in the absence of ACKR1 on NECs might also exit circulation, spleen apart, into the skin, gut and other tissues. BM sinusoids express ACKR1 but did not support the preferential homing of altered neutrophils. This might be explained by neutrophils using an alternative chemokine pathway for their homing to the BM shown to involve CXCR4 and CXCL1237, not an ACKR1–cognate chemokine46.

The uncovered here peculiarities of hematopoiesis taking place in the absence of ACKR1 on NECs are highly relevant for human health as Duffy-negative individuals of African ancestry selectively lack ACKR1 expression in the erythroid lineage only, but express it in ECs25. Neutrophils of the Duffy-negative individuals mirror the distinct molecular signature of neutrophils in ACKR1-deficient mice. We suggest that these altered neutrophils also readily leave circulation thus leading to neutropenia associated with the rs2814778(G) ACKR1 polymorphism23. It is conceivable that the differential signature of molecular effectors on neutrophils provided Duffy-negative individuals with a natural selective advantage for superior innate responses to microbial pathogens. Selective pressure by a broad range of infectious diseases, together with the known partial resistance of Duffy-negative individuals to *P. vivax* malaria47,48, may have contributed to the selection and fixation of the rs2814778(G) ACKR1 polymorphism in virtually entire population of Sub-Saharan Africa25.

In summary, we show that the absence of erythroid ACKR1 changes the steady-state hematopoiesis and alternative physiological patterns of hematopoiesis exist depending on ACKR1 expression in the erythroid lineage. In the future it will be intriguing to elucidate how ACKR1 expression by NECs might impact on emergency hematopoiesis and BM responses in infection, inflammation, injury and cancer.

Online Methods

Mice

ACKR1-deficient mice (Ref. 30) were backcrossed for more than 12 generations onto a C57BL/6J background and maintained as a heterozygous breed. Wild-type and ACKR1-deficient littermates were used for comparative studies. Mice were housed in specific pathogen-free facilities at the Universities of Birmingham and York, UK, LMU Munich, Germany, BMWF, Austria and CNIC, Madrid, Spain. All experimental procedures were performed with 8–12-week-old female mice, as approved by the respective Institutional Ethics and Animal Welfare Committees, Home Office, UK, or Regierung von Oberbayern, Munich, Germany, and compliant with UK, German, Spanish, Austrian and European Union guidelines.

Immunofluorescence staining and detection of ACKR1

Femurs were collected, cleaned and both ends cut off to facilitate the fixation in PFA (4%) overnight at 4°C. Bones were washed and decalcified in PBS with EDTA (10%) for 3 days, washed and incubated in 20% sucrose PBS overnight at 4°C, and finally embedded in OCT and stored at –80 °C. Sections (7 μm) were cut and blocked in 20% goat serum plus 0.5% Triton X-100 in PBS for 30 min at 20°C. After washing, sections were stained with rat anti-mouse CD31 antibody in PBS with 0.1% BSA, and secondary goat anti-rat AF488 was added. Finally, sections were stained with directly conjugated antibodies to mouse Ter119 (AF647) and mouse ACKR1 (AF546) for 1 h and washed with PBS. Slides were mounted in ProLong Gold anti-fade with DAPI for imaging. Evaluation was performed on a LSM880 (Zeiss).

Spleens were frozen in OCT on dry ice and 7 μm sections were cut on a cryomicrotome. Before staining, slides were air-dried for 30 min and fixed in acetone for 10 min. Slides were washed in PBS shortly and subsequently blocking with 20% goat serum in 0.1%BSA/PBS was performed. Antibodies against DARC (AF546), MECA-32 (AF647) and Ter119 (FITC) were diluted in 0.1% BSA in PBS and incubated on slides for 60 min. After three washes in PBS, slides were dipped in dH_2O, mounted with Prolong Gold with DAPI and evaluated as above.

Flow cytometry

To obtain BM cells, femurs were flushed with PBS and cells were washed with FACS buffer (PBS with 0.5% BSA). Fc receptors were blocked by rat antibody to mouse CD16/CD32 (2.4G2; BD Bioscience), where appropriate. In all experiments, antibody staining was performed at 4 °C for 60 min. Cells were counted using CountBright Absolute Counting Beads (Life Technologies), and were analyzed using a FACS CANTOII or LSR Fortessa flow cytometers (BD Biosciences) and FlowJo software (TreeStar). Details regarding antibodies used in flow cytometry and immunofluorescence staining are provided in Supplementary Table 1.

ACKR1 expression in BM cells

NECs were stained with antibodies to CD71 and Ter119. Stages of erythropoiesis were defined as follows: $CD71^{hi}$ $Ter119^{int}$ (population I, proerythroblasts), $CD71^{hi}$ $Ter119^{hi}$ forward scatter $(Fsc)^{hi}$ (population II, early normoblast), $CD71^{hi}$ $Ter119^{hi}$ $Fsc^{int/lo}$ (population III, intermediate normoblasts), $CD71^{hi/int}$ $Ter119^{hi}$ Fsc^{lo} (population IV, late normoblasts), $CD71^{int}$ $Ter119^{hi}$ Fsc^{lo} (population V, reticulocytes) and $CD71^{lo}$ $Ter119^{hi}$ Fsc^{lo} (population VI, mature erythrocytes). Fig. 1b provides details of the gating strategy. In addition, BM leukocytes were gated as Lineage (CD11b, Gr1, CD3, $B220)^{+}$ $CD71^{-}$ $Ter119^{-}$ cells. HSPCs were stained as described below. Expression of ACKR1 in NECs, leukocytes and HSPC was determined using the monoclonal anti-mouse ACKR1 antibody. ACKR1 expression was calculated in each erythoid cell population as specific delta mean fluorescence intensity (ΔMFI) = MFI in wild-type mouse minus average MFI in KO group. Data were then normalized to MEP and expressed as fold change.

Europe PMC Funders Author Manuscripts

HSPC analysis

For HSPC analysis, BM cells were stained with combinations of antibodies to the following surface markers: c-Kit, Sca-1, CD150, CD48, Flt3, CD34, CD16/32, IL-7ra and the lineage markers Ter119, B220, CD3, CD11b and Gr1. HSPCs were defined as follows:

HSC (Lineage$^-$ Sca1$^+$c-Kit$^+$CD48$^-$CD150$^+$Flt3$^-$);

MPP1a (Lineage$^-$ Sca1$^+$ c-Kit$^+$ CD48$^-$ CD150$^-$ Flt3$^-$);

MPP1b (Lineage$^-$ Sca1$^+$ c-Kit$^+$ CD48$^-$ CD150$^-$ Flt3$^+$);

MPP2 (Lineage$^-$ Sca1$^+$c-Kit$^+$CD48$^+$CD150$^+$Flt3$^-$);

LRP1 (Lineage$^-$ Sca1$^+$c-Kit$^+$CD48$^+$CD150$^-$Flt3$^-$);

LRP2 (Lineage$^-$ Sca1$^+$c-Kit$^+$CD48$^+$CD150$^-$Flt3$^+$);

CMP (Lineage$^-$ Sca1$^-$c-Kit$^+$CD34$^+$ CD16/32$^-$);

GMP (Lineage$^-$ Sca1$^-$c-Kit$^+$CD34$^+$ CD16/32$^+$);

MEP (Lineage$^-$ Sca1$^-$c-Kit$^+$CD34$^-$ CD16/32$^-$) and

CLP (Lineage$^-$ Sca1^{lo} c-Kit^{lo} IL-7ra$^+$ Flt3$^+$).

Neutrophil analysis

For surface markers and chemokine receptors expression analysis on neutrophils, BM cells were collected as above and blood cells were obtained by cardiac puncture in EDTA as an anticoagulant. Erythrocytes were lysed using ACK lysing buffer and cells washed with FACS buffer. Cells were reacted with antibodies to CD45, CD11b, Ly6G, CD16/32, CD62L, CD11a, CXCR2, CCR1, CCR2, CCR3 and CCR5.

Chemokine binding assay

BM cells were incubated with A647-conjugated CCL2 (10 nM, Almac) for 1 h at 37 °C and some cells were subsequently incubated with an excess of CXCL1 (1 μM) in PBS for 1 h to displace CCL2 or PBS alone. Cells were washed, stained for NEC markers using antibodies to CD71 and Ter119, and analyzed by flow cytometry. Specific binding of CCL2 was calculated for individual erythroid cell populations as ΔMFI of CCL2-A647 in wild-type and KO groups, normalized for the ACKR1-KO mature erythrocytes (population VI) and expressed as fold change.

Analysis of HSC-NEC interactions by flow cytometry

For observations of HSC-NEC interaction, mice were euthanized and perfused with PFA via cardiac route in order to fix the cells *in situ* and preserve their interactions. BM cells were collected and stained with the following antibody panel: c-Kit, Sca-1, CD150, CD48, CD71 and Ter119 and the lineage markers B220, CD3, CD11b and Gr1. The HSCs (LSK CD48$^-$CD150$^+$), MPP1 (LSK CD48$^-$ CD150$^-$), MPP2 (LSK CD48$^+$CD150$^+$) and LRP

Europe PMC Funders Author Manuscripts

(LSK CD48^{+} CD150^{-}) were gated and their interaction with NECs was assessed by the presence of costaining with CD71 and Ter119 on the duplets.

Blood erythrocyte and BM NEC parameters

Blood was taken by cardiac puncture and erythrocyte counts, hematocrit and hemoglobin concentration were determined using an automated ABX Pentra 60 blood counter (HORIBA ABX S.A.S). For BM analysis, mice were culled and flushed with PBS to remove erythrocytes present within the blood vessels. BM was harvested and different stages of erythropoiesis were analyzed as above.

Cell parameters in BM and blood

For BM leukocyte analysis the cells were stained with combinations of antibodies to the following surface markers: CD11b, Ly6G, CD115, CD19, B220. Leukocyte populations were defined as follows:

PMN (CD11b^{+}Ly6G^{+});

Monocytes (CD11b^{+}Ly6G^{-} CD115^{+});

B lineage (B220^{+}CD19^{-}).

Blood was taken by cardiac puncture and platelet counts were determined using an automated ABX Pentra 60 blood counter (HORIBA ABX S.A.S.). In addition, erythrocytes were lysed using ACK lysing buffer and cells washed with FACS buffer. Cells were reacted with antibodies to CD45, CD11b, Ly6G, CD115, CD3 and B220. Leucocyte populations were defined as follows:

PMN (CD11b^{+}Ly6G^{+});

Monocytes (CD11b^{+}Ly6G^{-}CD115^{+});

Lymphoid cells (B220^{+} CD3^{+}).

Cell proliferation

To assess the proliferation of BM cell populations, the APC BrdU flow kit (BD Bioscience) was used as per the manufacturer's instructions. Briefly, 5-bromo-2′ deoxyuridine (BrdU) was injected i.p. (1 mg) into wild-type and ACKR1-deficient mice. After 2 h, mice were euthanized, BM collected and labeled with a cocktail of biotinylated lineage antibodies followed by labeling with Anti-Biotin MicroBeads (Miltenyi Biotec) as per the manufacturer's instructions. Lineage^{+} BM cells were depleted and lineage^{-} BM cells were incubated with streptavidin (e450, eBioscience,) and with fluorescently labeled antibodies to c-Kit and Sca-1 for 1 h on ice. Cells were washed, fixed, permeabilized, stained with anti-BrdU antibody and analyzed by flow cytometry.

Reciprocal irradiation BM chimeric mice

BM cells from either C57BL/6 (wild-type) or ACKR1-deficient mice (KO) were harvested and transplanted into lethally irradiated (9 Gy) wild-type or ACKR1-deficient recipients by tail vein injection of 10^7 cells in 200 μl PBS, thus creating four experimental groups. Recipients received prophylactic endofloxacin (Baytril, Bayer AG) for a week prior to and also after irradiation. Eight weeks after the BM transfer the recipients were culled. BM and blood cells were collected, washed and stained to identify HSPCs and PMNs, respectively, as described above. The degree of donor chimerism was established by measuring the expression of ACKR1 on BM NECs and blood erythrocytes using anti-mouse ACKR1 antibody. In addition, CD45.1 and CD45.2 staining showed that all irradiated recipients BM HSPCs and blood PMNs were replaced by donor cells.

Parabiosis

To generate parabiotic pairs, we followed published protocols (49). Briefly, anesthetized mice were shaved at the corresponding lateral aspects and matching skin incisions were made from the olecranon to the knee joint of each mouse, and the subcutaneous fascia was bluntly dissected to create about 0.5 cm of free skin. The olecranon and knee joints were attached by a single 5-0 polypropylene suture and tie, and the dorsal and ventral skins were approximated by continuous suture. A single dose of flunixin meglumine (Schering-Plough) was injected subcutaneously in each partner at the end of the surgical procedure (1 mg/kg). Wild-type/wild type, KO/KO and wild-type/KO pairs were created. One month after surgery blood and BM were obtained from each of the partners for analysis of hematopoietic progenitors.

In another experiment where the homing of neutrophils was studied, different parabiotic pairs were undertaken: wild-type/wild type pairs (CD45.1 and CD45.2) and wild-type/KO pairs (CD45.1 and CD45.2 respectively). One month after surgery, blood, BM, spleen, lung and liver samples were obtained from each of the partners for analysis of neutrophils. Percentage of neutrophils from partner parabionts (percent chimerism) was defined on gated neutrophils in blood, BM, lung, liver and spleen. Migration indices were calculated for each tissue as the percent chimerism in a specific tissue divided by the percent chimerism in blood and normalised by using the values obtained in wild-type/wild type control pairs.

Cell sorting

BM of wild-type or ACKR1-deficient mice was flushed, cells were pooled from three mice and stained with lineage CD34, CD16/CD32, cKit, Sca-1 in 500 μl buffer, for 1 h on ice. Cells were sorted on a Mo-flow MultiLaser flow cytometer (Beckman Coulter). First, an enrichment step was performed, with gates set based on forward- and side- scatter characteristics for lineage-negative and either GMP cells or LSK cells. The GMP and LSK populations then underwent a second sorting step using the same gating profiles. The twice-sorted GMP and LSK populations, determined to be more than 97% pure, were snap frozen on dry ice for storage at -80 °C until used.

Europe PMC Funders Author Manuscripts

Microarray and analysis

RNA was extracted from sorted GMP and LSK populations using Trizol (Life Technologies) as per manufacturer's directions. Sample RNA (25 ng) was labelled with Cy3 dye as per the protocol detailed in the Low Input Quick Amp Labelling Kit (Agilent Technologies). A specific activity of greater than 6.0 was confirmed by measurement of 260 nm and 550 nm wavelengths with a NanoDrop ND-1000 Spectrophotometer. Labelled RNA (600 ng) was hybridized for 16 h to Agilent SurePrint G3 mouse 8x60K microarray slides. Slides were washed and scanned with a High Resolution C Scanner (Agilent Technologies), using a scan resolution of 3 μm. Feature extraction was performed using Agilent Feature Extraction Software, with no background subtraction. Scanned microarray images were analyzed using Agilent's Feature Extraction software. Feature intensities were background-subtracted according to the normal-exponential convolution model and normalized using 75th percentile normalization. Differentially expressed genes were identified using Significant Analysis of Microarrays (SAM) method with FDR<0.05 using Multiexperiment Viewer (MeV) software (http://www.tm4.org/mev.html). Hierarchical clustering was obtained using Gene Cluster3.0 software.

In order to ascribe characteristic profiles to the set of genes differentially expressed in the microarray analysis, the specificity of genes upregulated in both LSK and GMP from KO mice, defined as Cluster 1, was determined based on their annotation in Gene Expression Commons (GEXC) (50). Briefly, the gene expression activity files of all BM cells were downloaded from GEXC (https://gexc.stanford.edu), aligned with the retrieved 69 genes of Cluster 1 and the heatmaps of their expression activity were created for individual cell populations. The analysis showed enrichment primarily in PMN-specific genes. To determine whether such enrichment was selective for a subset or PMN genes, the expression of all genes annotated as PMN-specific in the Immgen database (http://www.immgen.org/) was assessed in the microarray. Briefly, among 334 defined cell-specific clusters in Immgen "Modules and Regulators" tool, three modules 209, 210 and 258 have been assigned as PMN-specific, encompassing 54 genes in total, 22, 11 and 12, respectively. The expression of these genes was verified in the microarray and presented for individual modules as heatmaps.

Two-photon laser scanning microscopy (TPLSM) of the whole mounted BM

Mice were euthanized and perfused via cardiac puncture with 3 ml cold PBS followed by 3 ml cold 4% paraformaldehyde (PFA). Femurs were harvested, carefully cleaned from the surrounding tissue and post-fixed in 4% PFA at 4°C overnight. After fixation, bones were shortly washed with PBS and cryopreserved in 15% sucrose at 4 °C for 2 h followed by incubation in 30% sucrose at 4 °C overnight. Bones were embedded into Optical Cutting Temperature (OCT) compound and flash-frozen. Samples were longitudinally shaved with a Leica CM3050S cryostat in order to expose the BM along the full femur length, OCT residues were washed away with PBS and non-specific antigens were blocked by a PBS solution containing 20% normal goat serum and CD16/CD32 Fc-block (final concentration 0.5 μg/ml) for 2 h at 20°C Bones were incubated overnight in the dark at 20°C with the following directly-conjugated antibodies: CD150, CD71 and Lineage (CD3, B22, Gr1, CD11b, CD48, CD41). After incubation, the bones were washed several times with PBS and

embedded into PBS-based 1.5% agarose gel prior to imaging. Further details regarding imaging reagents are provided in Supplementary Table 1.

Four-color TPLSM microscopy was performed on a Leica SP5IIMP equipped with a 20X NA1.00 WD objective (Leica) and a pre-chirped MaiTai Ti:Sa pulsed laser (Spectra-Physics) tuned at 800 nm to maximize dye emission. Optical zoom was applied where applicable. To allow the simultaneous collection of all spectra while minimizing color spillover, the collection channels of Hybrid diode detectors were determined as follows: 380-415 nm for bone-collagen-derived SHG signal, 420-470 nm for Pacific Blue, 500-550 nm for Alexa Fluor 488 and 600-650 nm for PE. *z*-stacks (1 μm step-size) of 1024x1024 pixel *xy* images (f.o.v. 356 x 356 μm^2) were collected up to 100-150 μm depth. *z*-stacks were 3D reconstructed using the Imaris software (Bitplane). HSCs were identified as $CD150^+Lin^-CD7^-$ cells and NECs as $CD71^+Lin^-CD150^-$ cells. Both stains were rendered as isosurface and distances between HSCs and the closest NECs were determined using the software's measurement tools.

Human population genetics

Allele frequencies for the autosomal SNP rs2814778 within different ethnic populations were retrieved from 1000 genomes project dataset using Ensembl (www.ensembl.org). The A and G alleles correspond to the adenine and guanine, respectively, at the position -43 within GATA-1-binding motif of the promoter of ACKR1 gene. Substitution from A to G results in the absence of ACKR1 expression in the erythroid lineage.

Human blood samples

Blood was collected from healthy individuals as approved by the ethical committee of LMU, Munich following written consent. To determine the expression of Duffy antigen on erythrocytes the whole blood was stained with mouse monoclonal anti-ACKR1 antibody (Fy6, gift from Dr. M. Uchikawa), washed and stained with a FITC-conjugated secondary antibody. For staining of neutrophil surface markers erythrocytes were lysed using ACK lysing buffer and cells washed with FACS buffer. Cells were reacted with antibodies to CD45, CD11b, CD16, CXCR1, CXCR2 and CCR2 analyzed using a FACS CANTO II flow cytometer.

Statistical analysis

Multiple independent experiments were performed to verify the reproducibility of experimental findings. When suitable, sample sizes were estimated based on results of explorative experiments in order to provide adequate power. No randomization or blinding was used in any experiments. Animals were excluded from experiments if they showed any signs of sickness. Differences in two group comparisons were assessed by unpaired Student's *t*-test, with Welch's correction when appropriate. Comparisons between three or more group were performed by One-Way or Two-Way ANOVA as appropriate, followed by Tukey's post-hoc test. Difference in proportions was assessed by χ^2 with Fisher's correction, when appropriate. Statistical significance is represented by asterisks and corresponding p=values as indicated in the legends. Data are expressed as mean values ±

SEM or mean values ± SD. Biological replicates are stated in the legends for each figure. Statistical analysis was performed with G-Power (51) and Prism6 (GraphPad) softwares.

Supplementary Material

Refer to Web version on PubMed Central for supplementary material.

Acknowledgement

Supported by the Medical Research Council grant (G0802838) and Senior Visiting Fellowship of the Center for Advanced Studies LMU, Munich to A.R; Wellcome Trust grant (WT090962MA) to I.N-B, A.R. and P.M; Deutsche Zentrum Für Herz-Kreislauf-Forschung (86X2600229) and Marie Curie Actions Intra-European Fellowship to J.D; Deutsche Forschungsgemeinschaft grants (SFB1123/A1 SFB1123/Z1, INST 409/150-1 FUGG) to C.W., M.B. and R.T.A.M; European Research Council grant (ERC AdG °692511) to CW; Swiss National Science Foundation Sinergia grant (CRSII3_160719) to E.H. and A.R; TransCard PhD fellowship in Translational Cardiovascular and Metabolic Medicine of the Helmholtz International Research School to K.N; ERA-EDTA Short-term fellowship to K.A.; AF2015-65607-R from MINECO to A.H. The CNIC is supported by the Ministry of Economy, Industry and Competitiveness (MINECO) and the Pro CNIC Foundation, and is a Severo Ochoa Center of Excellence (MINECO award). We are in debt to M. Ulvmar, E. Ross, G. Volpe, P. Cauchy and A. Cunningham for their advice, R. Bird and S. Kissane for their assistance with cell sorting and microarray, respectively, H. Vyas and P. Kelay for help with laboratory work and D. Santovito for help with statistical analysis. We thank Prof. M. Mack (University of Regensburg) and Dr. M. Uchikawa (Japanese Red Cross) for their generous gifts of anti-mouse CCR2 antibody and anti-human ACKR1 antibody, respectively, Profs. J. Allen (University of Manchester) and M. Bader (Max Delbruck Center) for critically reading the manuscript and their suggestion. A.R. is grateful to Ms. M. Tsaloumas, Mr. A. Denniston and Mr. N. Glover for the vision.

References

1. Rot A, von Andrian UH. Chemokines in innate and adaptive host defense: basic chemokinese grammar for immune cells. Annual review of immunology. 2004; 22:891–928.
2. Griffith JW, Sokol CL, Luster AD. Chemokines and chemokine receptors: positioning cells for host defense and immunity. Annual review of immunology. 2014; 32:659–702.
3. Luther SA, Cyster JG. Chemokines as regulators of T cell differentiation. Nature immunology. 2001; 2:102–107. [PubMed: 11175801]
4. Krathwohl MD, Kaiser JL. Chemokines promote quiescence and survival of human neural progenitor cells. Stem Cells. 2004; 22:109–118. [PubMed: 14688397]
5. Ulvmar MH, Hub E, Rot A. Atypical chemokine receptors. Experimental cell research. 2011; 317:556–568. [PubMed: 21272574]
6. Bachelerie F, et al. New nomenclature for atypical chemokine receptors. Nature immunology. 2014; 15:207–208. [PubMed: 24549061]
7. Nibbs RJB, Graham GJ. Immune regulation by atypical chemokine receptors. Nature Reviews Immunology. 2013; 13:815–829.
8. Bachelerie F, et al. International Union of Basic and Clinical Pharmacology. [corrected]. LXXXIX. Update on the extended family of chemokine receptors and introducing a new nomenclature for atypical chemokine receptors. Pharmacol Rev. 2014; 66:1–79. [PubMed: 24218476]
9. Pruenster M, et al. The Duffy antigen receptor for chemokines transports chemokines and supports their promigratory activity. Nature immunology. 2009; 10:101–108. [PubMed: 19060902]
10. Ulvmar MH, et al. The atypical chemokine receptor CCRL1 shapes functional CCL21 gradients in lymph nodes. Nature immunology. 2014; 15:623–630. [PubMed: 24813163]
11. Lee KM, et al. The chemokine receptors ACKR2 and CCR2 reciprocally regulate lymphatic vessel density. The EMBO journal. 2014; 33:2564–2580. [PubMed: 25271254]
12. Cruz-Orengo L, et al. CXCR7 influences leukocyte entry into the CNS parenchyma by controlling abluminal CXCL12 abundance during autoimmunity. The Journal of experimental medicine. 2011; 208:327–339. [PubMed: 21300915]

13. Novitzky-Basso I, Rot A. Duffy antigen receptor for chemokines and its involvement in patterning and control of inflammatory chemokines. Frontiers in immunology. 2012; 3:266. [PubMed: 22912641]
14. Rot A. Contribution of Duffy antigen to chemokine function. Cytokine & growth factor reviews. 2005; 16:687–694. [PubMed: 16054417]
15. Mei J, et al. CXCL5 regulates chemokine scavenging and pulmonary host defense to bacterial infection. Immunity. 2010; 33:106–117. [PubMed: 20643340]
16. Schnabel RB, et al. Duffy antigen receptor for chemokines (Darc) polymorphism regulates circulating concentrations of monocyte chemoattractant protein-1 and other inflammatory mediators. Blood. 2010; 115:5289–5299. [PubMed: 20040767]
17. Reutershan J, Harry B, Chang D, Bagby GJ, Ley K. DARC on RBC limits lung injury by balancing compartmental distribution of CXC chemokines. European journal of immunology. 2009; 39:1597–1607. [PubMed: 19499525]
18. Miller LH, Mason SJ, Dvorak JA, McGinniss MH, Rothman IK. Erythrocyte receptors for (Plasmodium knowlesi) malaria: Duffy blood group determinants. Science. 1975; 189:561–563. [PubMed: 1145213]
19. Horuk R, et al. A receptor for the malarial parasite Plasmodium vivax: the erythrocyte chemokine receptor. Science. 1993; 261:1182–1184. [PubMed: 7689250]
20. Nedelec Y, et al. Genetic Ancestry and Natural Selection Drive Population Differences in Immune Responses to Pathogens. Cell. 2016; 167:657–669 e621. [PubMed: 27768889]
21. Quach H, et al. Genetic Adaptation and Neandertal Admixture Shaped the Immune System of Human Populations. Cell. 2016; 167:643–656 e617. [PubMed: 27768888]
22. Thobakgale CF, Ndung'u T. Neutrophil counts in persons of African origin. Curr Opin Hematol. 2014; 21:50–57. [PubMed: 24257098]
23. Reich D, et al. Reduced neutrophil count in people of African descent is due to a regulatory variant in the Duffy antigen receptor for chemokines gene. PLoS Genet. 2009; 5:e1000360. [PubMed: 19180233]
24. Sanger R, Race RR, Jack J. The Duffy Blood Groups of New-York Negroes - the Phenotype Fy (a-B-). Brit J Haematol. 1955; 1:370–374. [PubMed: 13269673]
25. Howes RE, et al. The global distribution of the Duffy blood group. Nature communications. 2011; 2:266.
26. Tournamille C, Colin Y, Cartron JP, Le Van Kim C. Disruption of a GATA motif in the Duffy gene promoter abolishes erythroid gene expression in Duffy-negative individuals. Nature genetics. 1995; 10:224–228. [PubMed: 7663520]
27. Peiper SC, et al. The Duffy antigen/receptor for chemokines (DARC) is expressed in endothelial cells of Duffy negative individuals who lack the erythrocyte receptor. The Journal of experimental medicine. 1995; 181:1311–1317. [PubMed: 7699323]
28. Doss JF, et al. A comprehensive joint analysis of the long and short RNA transcriptomes of human erythrocytes. BMC Genomics. 2015; 16:952. [PubMed: 26573221]
29. Thiriot A, Perdomo C, Cheng G, Novitzky-Basso I, McArdle S, Barreiro O, Mazo I, Triboulet R, Ley K, Rot A, von Andrian UH. Differential immunostaining of DARC/ACKR1 distinguishes venular from non-venular endothelial cells in murine tissues. BMC Biology. (in press).
30. Dawson TC, et al. Exaggerated response to endotoxin in mice lacking the Duffy antigen/receptor for chemokines (DARC). Blood. 2000; 96:1681–1684. [PubMed: 10961863]
31. Itkin T, et al. Distinct bone marrow blood vessels differentially regulate haematopoiesis. Nature. 2016; 532:323–328. [PubMed: 27074509]
32. Morrison SJ, Scadden DT. The bone marrow niche for haematopoietic stem cells. Nature. 2014; 505:327–334. [PubMed: 24429631]
33. Mendelson A, Frenette PS. Hematopoietic stem cell niche maintenance during homeostasis and regeneration. Nature medicine. 2014; 20:833–846.
34. Fossati G, Moots RJ, Bucknall RC, Edwards SW. Differential role of neutrophil Fcgamma receptor IIIB (CD16) in phagocytosis, bacterial killing, and responses to immune complexes. Arthritis Rheum. 2002; 46:1351–1361. [PubMed: 12115243]

35. Gao H, Henderson A, Flynn DC, Landreth KS, Ericson SG. Effects of the protein tyrosine phosphatase CD45 on FcgammaRIIa signaling and neutrophil function. Exp Hematol. 2000; 28:1062–1070. [PubMed: 11008019]
36. Minten C, et al. DARC shuttles inflammatory chemokines across the blood-brain barrier during autoimmune central nervous system inflammation. Brain : a journal of neurology. 2014; 137:1454–1469. [PubMed: 24625696]
37. Martin C, et al. Chemokines acting via CXCR2 and CXCR4 control the release of neutrophils from the bone marrow and their return following senescence. Immunity. 2003; 19:583–593. [PubMed: 14563322]
38. Busch K, et al. Fundamental properties of unperturbed haematopoiesis from stem cells in vivo. Nature. 2015; 518:542–546. [PubMed: 25686605]
39. Yu VW, et al. Epigenetic Memory Underlies Cell-Autonomous Heterogeneous Behavior of Hematopoietic Stem Cells. Cell. 2016; 167:1310–1322 e1317. [PubMed: 27863245]
40. Sun J, et al. Clonal dynamics of native haematopoiesis. Nature. 2014; 514:322–327. [PubMed: 25296256]
41. Pietras EM, et al. Functionally Distinct Subsets of Lineage-Biased Multipotent Progenitors Control Blood Production in Normal and Regenerative Conditions. Cell Stem Cell. 2015; 17:35–46. [PubMed: 26095048]
42. Bandyopadhyay S, et al. Interaction of KAI1 on tumor cells with DARC on vascular endothelium leads to metastasis suppression. Nature medicine. 2006; 12:933–938.
43. Hur J, et al. CD82/KAI1 Maintains the Dormancy of Long-Term Hematopoietic Stem Cells through Interaction with DARC-Expressing Macrophages. Cell Stem Cell. 2016; 18:508–521. [PubMed: 26996598]
44. Youn BS, Mantel C, Broxmeyer HE. Chemokines, chemokine receptors and hematopoiesis. Immunological reviews. 2000; 177:150–174. [PubMed: 11138773]
45. Sugiyama T, Kohara H, Noda M, Nagasawa T. Maintenance of the hematopoietic stem cell pool by CXCL12-CXCR4 chemokine signaling in bone marrow stromal cell niches. Immunity. 2006; 25:977–988. [PubMed: 17174120]
46. Gardner L, Patterson AM, Ashton BA, Stone MA, Middleton J. The human Duffy antigen binds selected inflammatory but not homeostatic chemokines. Biochemical and biophysical research communications. 2004; 321:306–312. [PubMed: 15358176]
47. Menard D, et al. Plasmodium vivax clinical malaria is commonly observed in Duffy-negative Malagasy people. Proceedings of the National Academy of Sciences of the United States of America. 2010; 107:5967–5971. [PubMed: 20231434]
48. Miller LH, Mason SJ, Clyde DF, McGinniss MH. The resistance factor to Plasmodium vivax in blacks. The Duffy-blood-group genotype, FyFy. N Engl J Med. 1976; 295:302–304. [PubMed: 778616]
49. Wright DE, Wagers AJ, Gulati AP, Johnson FL, Weissman IL. Physiological migration of hematopoietic stem and progenitor cells. Science. 2001; 294:1933–1936. [PubMed: 11729320]
50. Seita J, Sahoo D, Rossi DJ, Bhattacharya D, Serwold T, Inlay MA, Ehrlich LIR, Fathman JW, Dill DL, Weissman IL, Esteban FJ. Gene Expression Commons: an open platform for absolute gene expression profiling. PloS one. 2012; 7:e40321. [PubMed: 22815738]
51. Faul F, Erdfelder E, Lang A-G, Buchner A. G. Power 3: A flexible statistical power analysis program for the social, behavioral, and biomedical sciences. Behavior Research Methods. 2007; 39:175–191. [PubMed: 17695343]
52. Mack M, Cihak J, Simonis C, Luckow B, Proudfoot AE, Plachy J, Bruhl H, Frink M, Anders HJ, Vielhauer V, Pfirstinger J, Stangassinger M, Schlondorff D. Expression and characterization of the chemokine receptors CCR2 and CCR5 in mice. The Journal of Immunology. 2001; 166:4697–4704. [PubMed: 11254730]

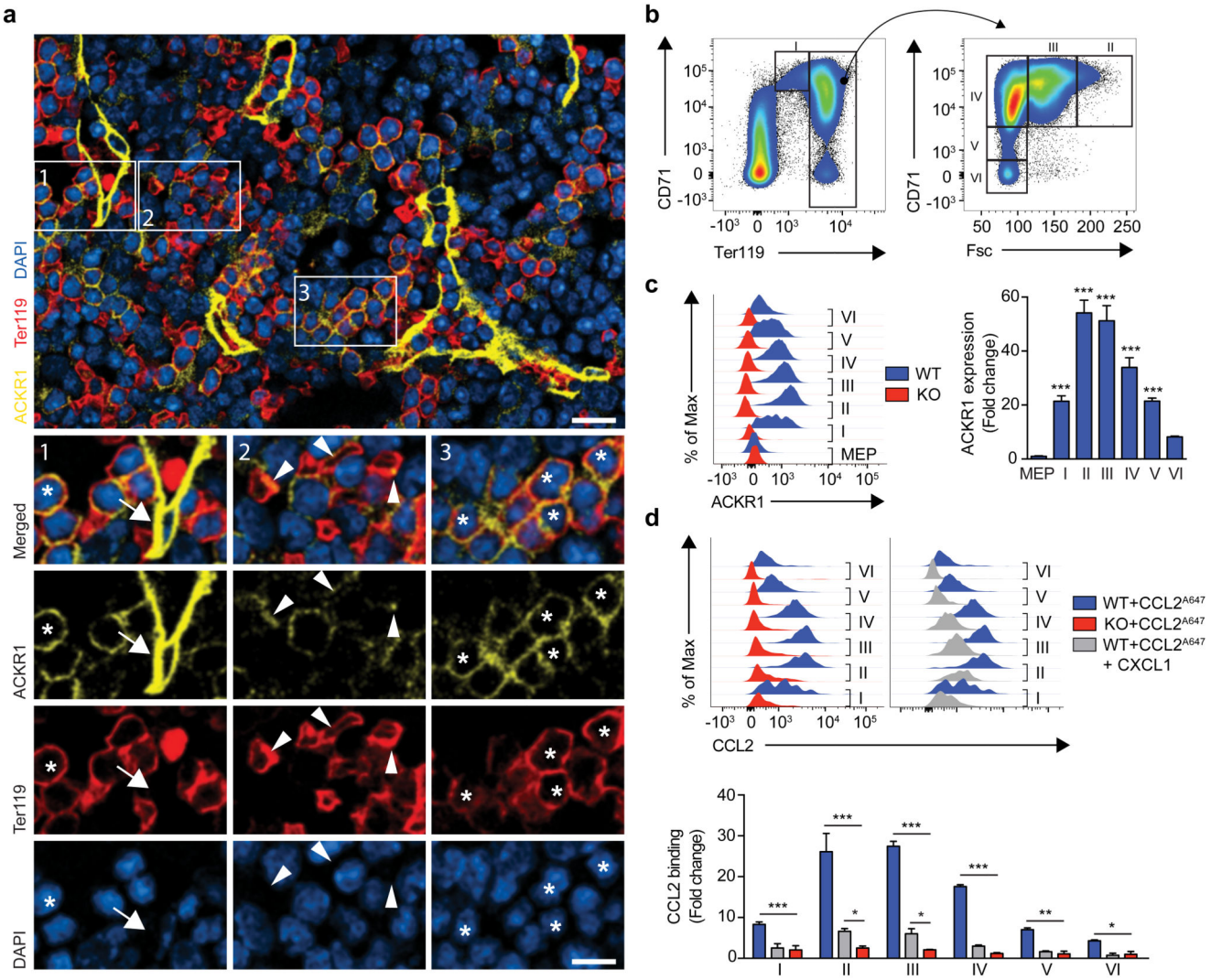

Fig. 1. ACKR1 is expressed in the BM by ECs and NECs.

(**a**) Immunofluorescence micrograph of wild-type BM stained with anti-ACKR1 (yellow), anti-Ter119 (red, erythroid cells) and DAPI (blue). Insets show ACKR1 immunoreactivity in sinusoidal EC (arrows), anuclear mature erythrocytes (arrowheads) and NECs (asterisks). Scale bars, 30 μm (main image) and 15 μm (insets). (**b**) BM flow cytometry to identify the stages of erythroid maturation; proerythroblasts (I), early normoblasts (II), intermediate normoblasts (III), late normoblasts (IV), reticulocytes (V) and mature red cells (VI) gated based on CD71, Ter119 and forward scatter (Fsc). (**c**) ACKR1 expression on megakaryocytic-erythroid progenitors (MEP) and erythroid cells (I-VI) in wild-type (blue) and ACKR1-deficient (red) BM. Left, representative flow cytometry histogram plots; right, quantitative analysis in wild-type BM expressed as fold change to MEP. Mean±SEM; n=6 from two independent experiments. One-way ANOVA; ***P < 0.01. (**d**) AF647-CCL2 binding to erythroid cells (I-VI) isolated from wild-type (blue) and ACKR1-deficient (red) BM and competition for AF647-CCL2 binding to wild-type erythroid cells by subsequent addition of unlabeled CXCL1 (grey). Top, representative flow cytometry histogram plots;

bottom, quantitative analysis expressed as fold change compared to binding to ACKR1-deficient erythrocytes. Mean±SD; n=2 from two independent experiments. Two-way ANOVA, * P<0.05, **P < 0.01, ***P < 0.001

Europe PMC Funders Author Manuscripts

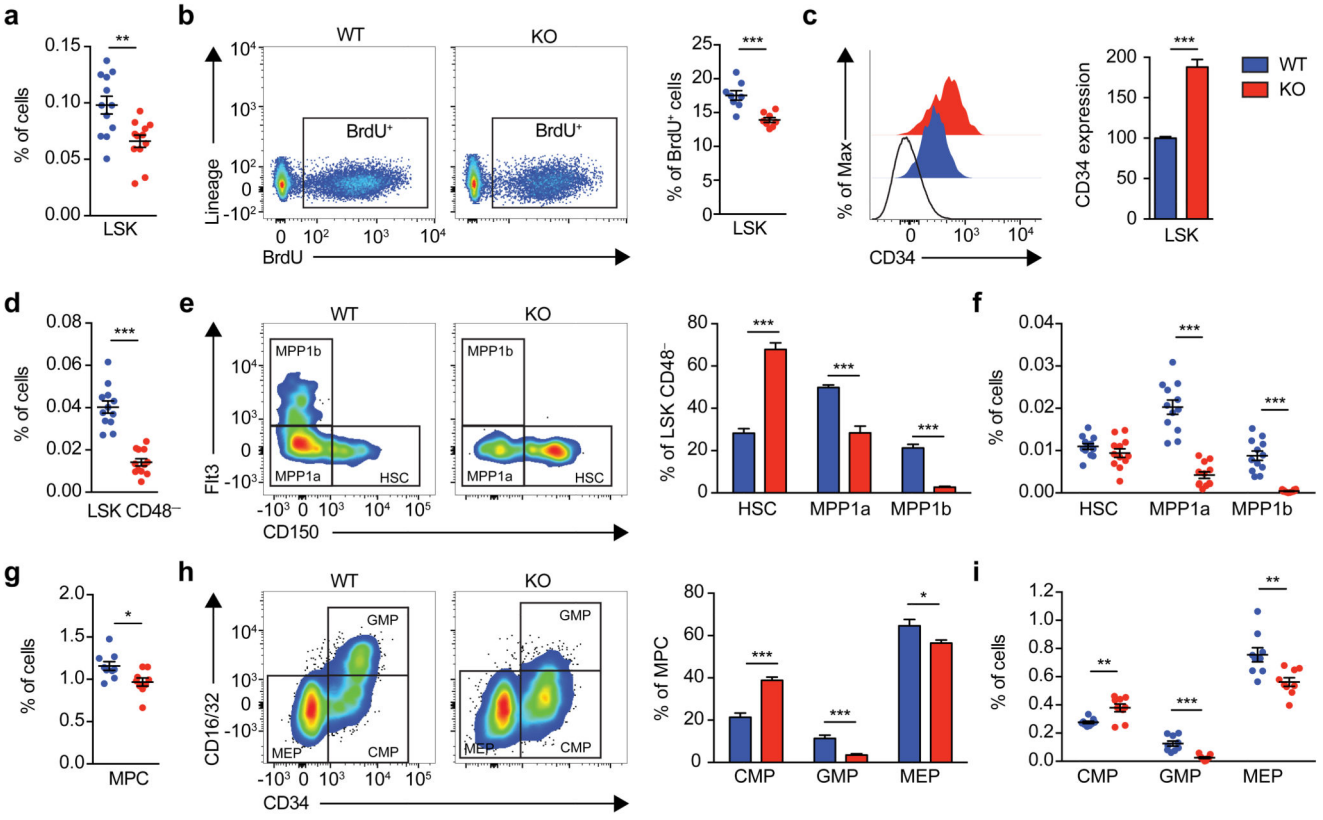

Fig. 2. ACKR1 deficiency alters HSPC populations.

(**a**) Frequency of LSKs in wild-type (WT; blue) and ACKR1-deficient (KO; red) BMs, (**b**) BrdU incorporation and (**c**) CD34 expression in LSK cells. (**d**) Frequency of LSK CD48⁻ cells and (**e**) relative distribution of their HSC, MPP1a and MPP1b subpopulations. (**f**) BM frequencies of HSC, MPP1a and MPP1b cells. (**g**) Frequency of MPCs and (**h**) distribution of their CMP, GMP and MEP subpopulations. (**I**) BM frequencies of CMP, GMP and MEP cells. (**a, c-f**) n=12 in four independent experiments. (**b**) n= 8 in two independent experiments. (**g-i**) n=9 in three independent experiments. All data show Mean±SEM. Two-tailed Student's t-test; *P < 0.05, **P < 0.01 and ***P < 0.001.

Europe PMC Funders Author Manuscripts

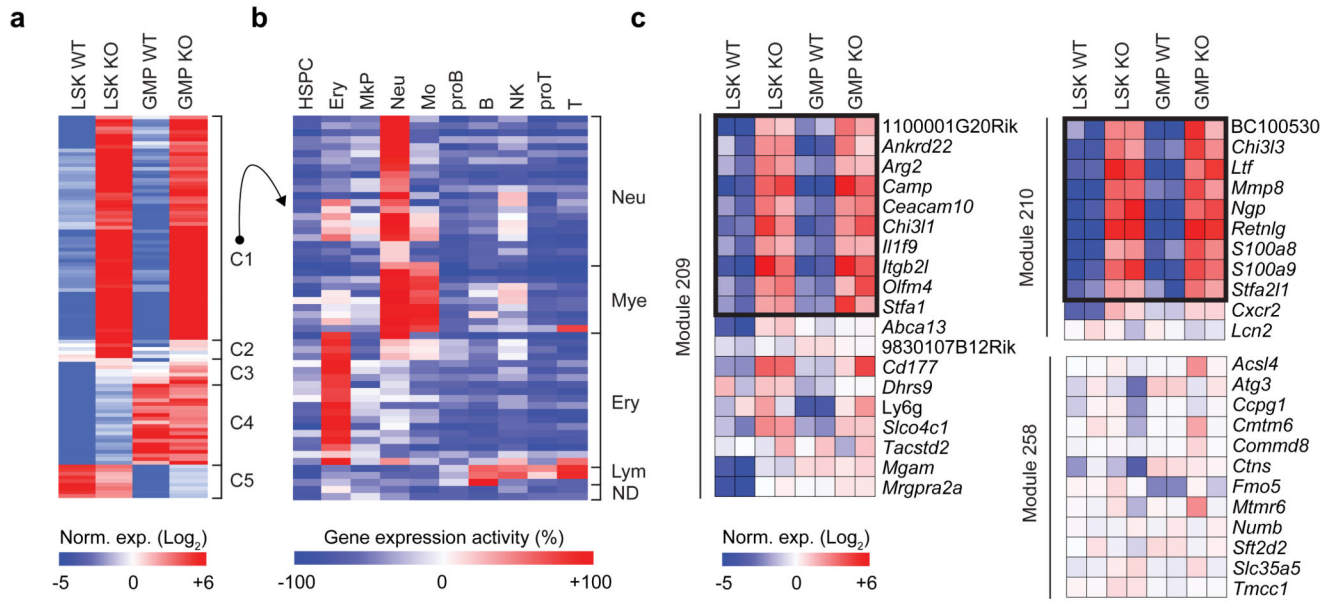

Fig. 3. ACKR1 deficiency changes HSPC transcriptomes.

(**a**) Microarray heatmap of gene expression in LSK and GMP populations from wild-type (WT) and ACKR1-deficient (KO) BM. (**b**) Genes from cluster 1 were analyzed for their expression activity in different BM cell types. Erythroid cells (Ery); Megakaryocyte progenitors (MkP); Neutrophils (Neu); Monocytes (Mo); B cell progenitors (proB); mature B cells (B); natural killer (NK); T cell progenitors (proT) and T cells (T). (**l**) Microarray heatmaps showing gene expression in three specific neutrophil-enriched modules. Black boxes indicate genes significantly upregulated in HSPC from AKCR1-deficient as compared to WT cells.

Europe PMC Funders Author Manuscripts

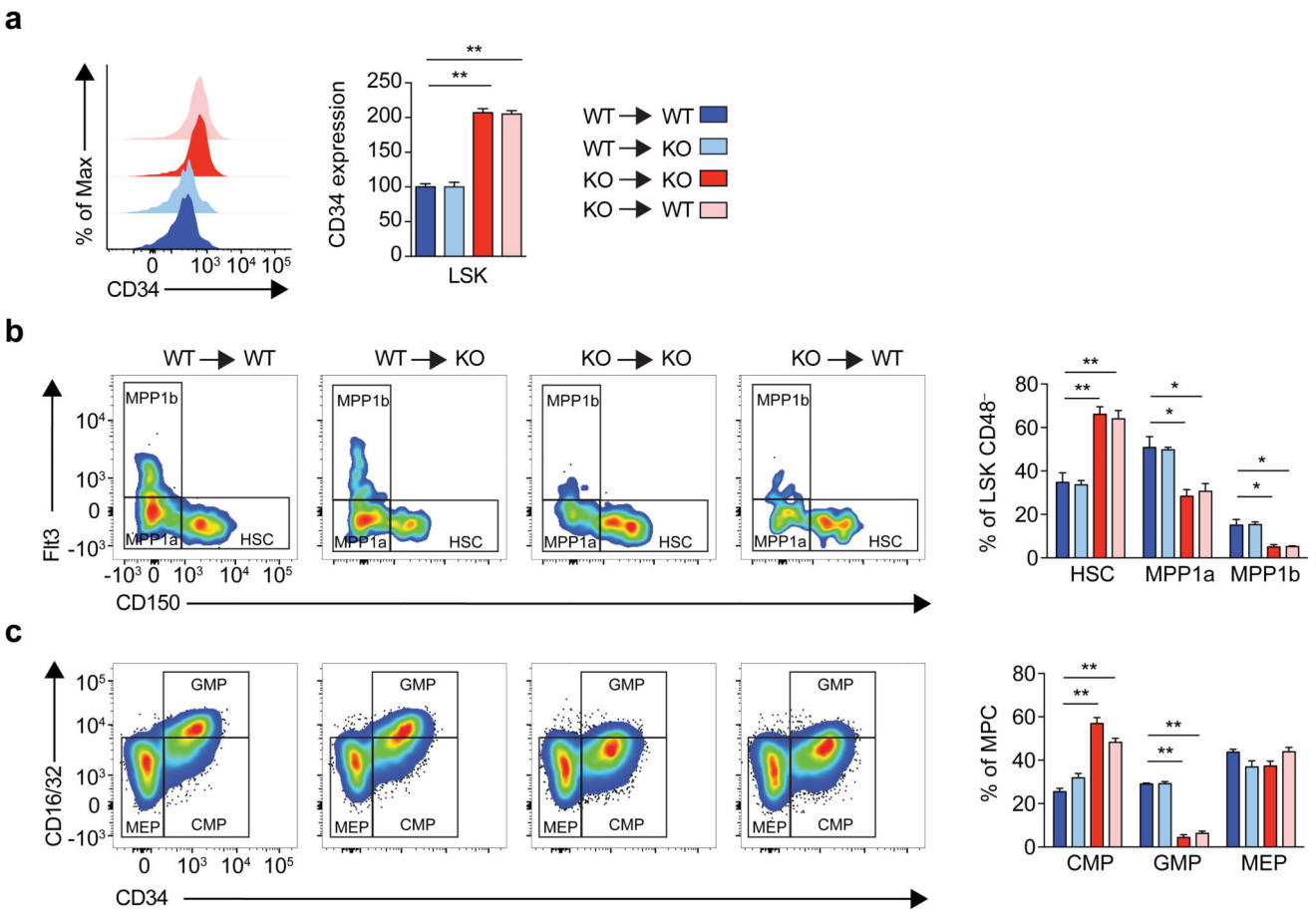

Fig. 4. ACKR1 on erythroid cells but not ECs regulates HSPCs.

(**a**) CD34 expression in LSK cells of BM chimeric mice; wild-type (WT) reconstituted into WT (blue), WT reconstituted into ACKR1-deficient (KO, light blue), KO reconstituted into KO (red) and KO reconstituted into WT (pink). Left, representative flow cytometry histogram plots; right, quantitative analysis. (**b-c**) Proportions of HSC, MPP1a and MPP1b subpopulations of LSK CD48⁻ cells (**b**) and CMP, GMP and MEP subpopulations of MPCs (**c**) in BM chimeric mice; Left, representative dot plots; right, quantitative analysis. . n=4 from two independent experiments. One-way ANOVA. All data are Mean±SEM., *P < 0.01 and **P < 0.001.

Europe PMC Funders Author Manuscripts

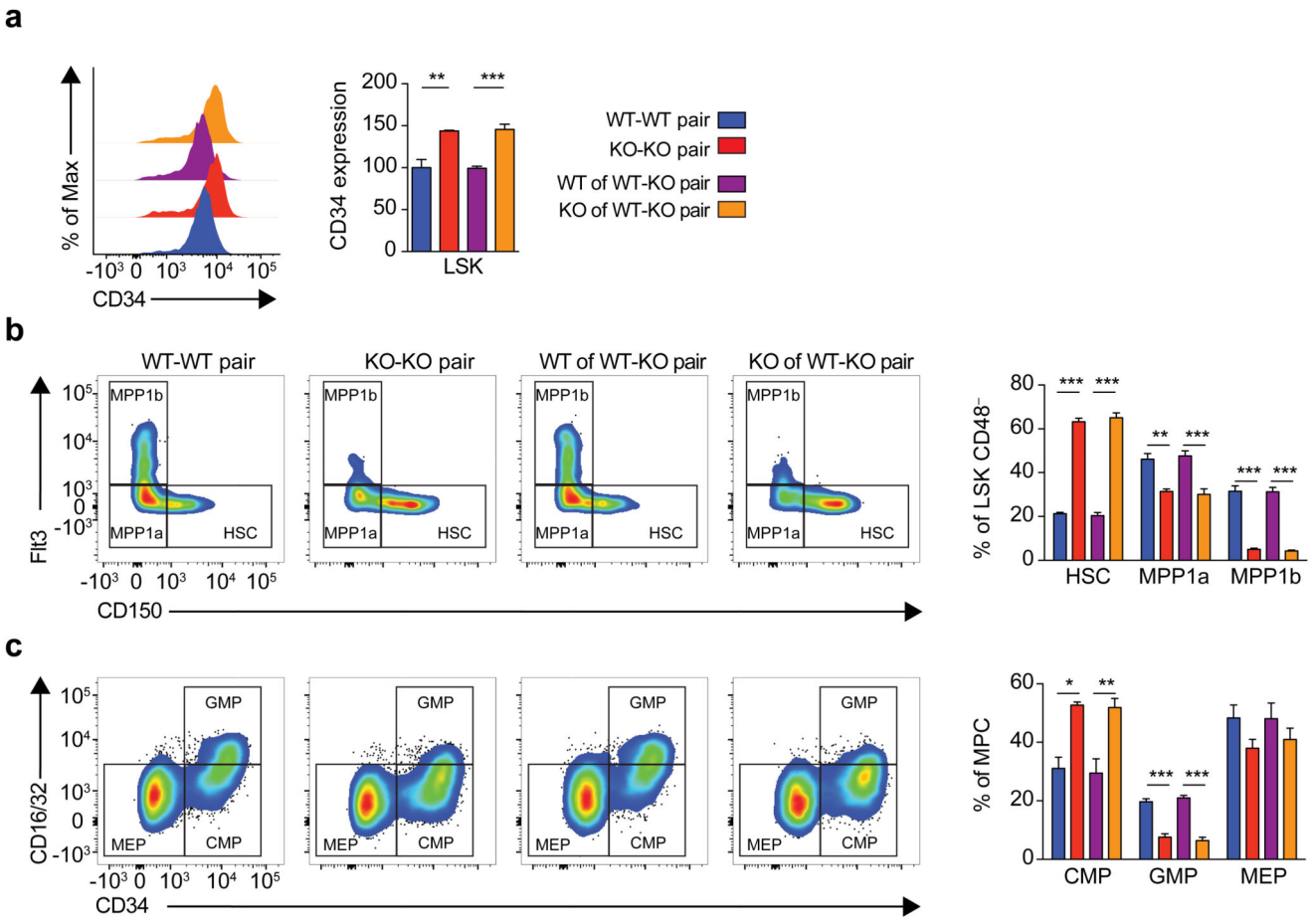

Fig. 5. ACKR1 on BM erythroid cells regulates HSPC.

(**a**) CD34 expression by LSK in parabiotic mice: wild-type (WT) with WT (blue), ACKR1-deficient (KO) with KO (red), WT in WT with KO parabiotic pair (purple) and KO in WT with KO parabiotic pair (orange). Left, representative flow cytometry histogram plots; right, quantitative analysis. (**b-c**) Proportions of HSC, MPP1a and MPP1b subpopulations of LSK CD48^{-} cells (**b**) and CMP, GMP and MEP subpopulations of MPCs (**c**) in BMs of parabiotic mice; Left, representative dot plots; right, quantitative analysis. n=4 from two independent experiments. One-way ANOVA. All data are Mean±SEM. *P < 0.05, **P < 0.01 and ***P < 0.001.

Europe PMC Funders Author Manuscripts

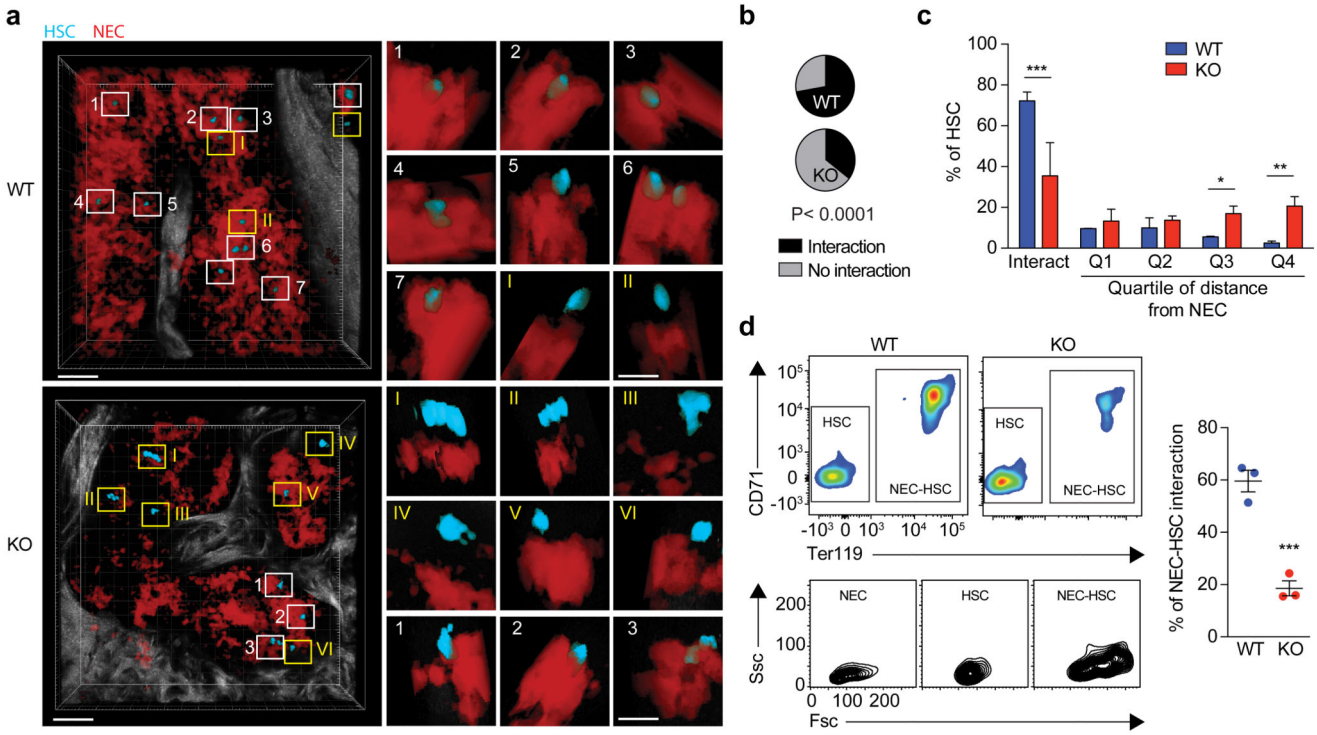

Fig. 6. ACKR1 on NECs promotes direct cell interactions with HSCs.

(**a**) BM localization of HSCs (blue) and NECs (red) in representative 3D-recontruction images from wild-type (WT) and ACKR1-deficient (KO) whole-mounted femurs assessed by two-photon microscopy. White squares with Arabic numerals mark cell contacts between a HSC and NECs; yellow squares with Roman numerals indicate HSCs not interacting with NECs. Scale bars, 50μm (main images) and 25μm (insets). (**b**) Proportions of NEC-interacting and non-interacting HSCs. Chi^2 ; $P < 0.0001$. (**c**) Distance between HSCs and NECs in WT (blue) and KO (red) BM. Among non-interacting HSCs, distribution quartiles were defined as: Q1, < 2.56μm, Q2, < 4.96μm, Q3, < 8.30μm and Q4, <19.82μm. Mean±SD. One-way ANOVA. (**b** and **c**) n=145 HSCs (WT) and 144 HSCs (KO) assessed by two-photon microscopy in two independent experiments. (**d**) HSC interactions with NECs (NEC-HSC) assessed by flow cytometry in wild-type (WT) and ACKR1-deficient (KO); left, representative dot-plots; right, quantitative analysis. Two-tailed Student's t-test, (n=3). Mean ±SEM. *P < 0.05, **P < 0.01 and ***P < 0.001.

Europe PMC Funders Author Manuscripts

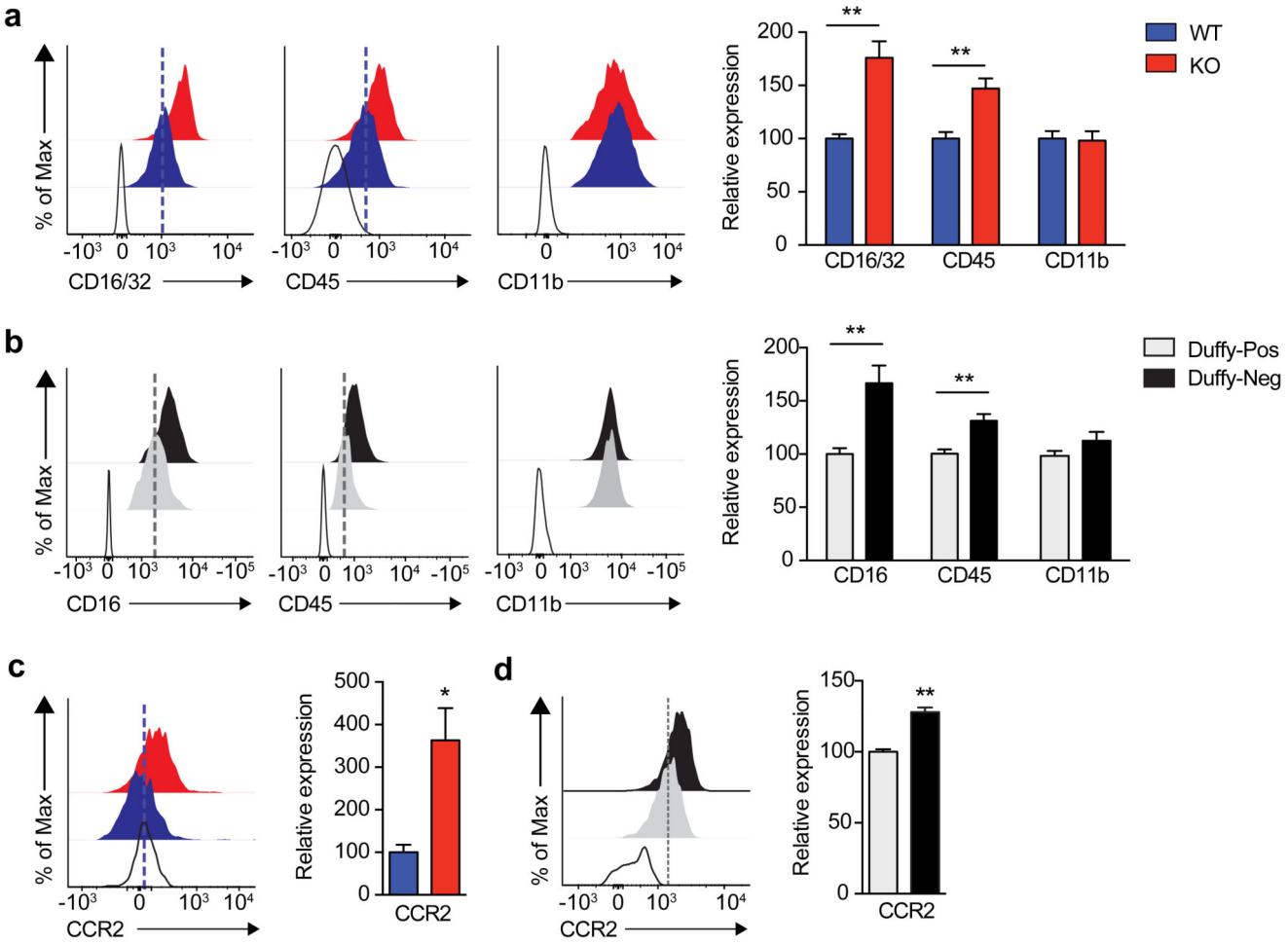

Fig. 7. Lack of ACKR1 affects neutrophil phenotype.

(**a**) Expression of CD16/32, CD45 and CD11b in blood neutrophils from wild-type (WT, blue) and ACKR1-deficient (KO, red) mice. n=9 from three independent experiments. (**b**) CD16, CD45 and CD11b expression in human blood neutrophils from healthy Duffy-positive (grey bars, n=14) and Duffy-negative (black bars, n=7) individuals from three independent experiments. (**c**) Expression of CCR2 in blood neutrophils from WT and KO mice. n=9 from four independent experiments. (**d**) Expression of CCR2 in human blood neutrophils from Duffy-positive (n=11) and Duffy-negative individuals (n=4) in three independent experiments. All data show Mean±SEM. two-tailed Student's t-test; *P < 0.01, **P < 0.001.

Europe PMC Funders Author Manuscripts

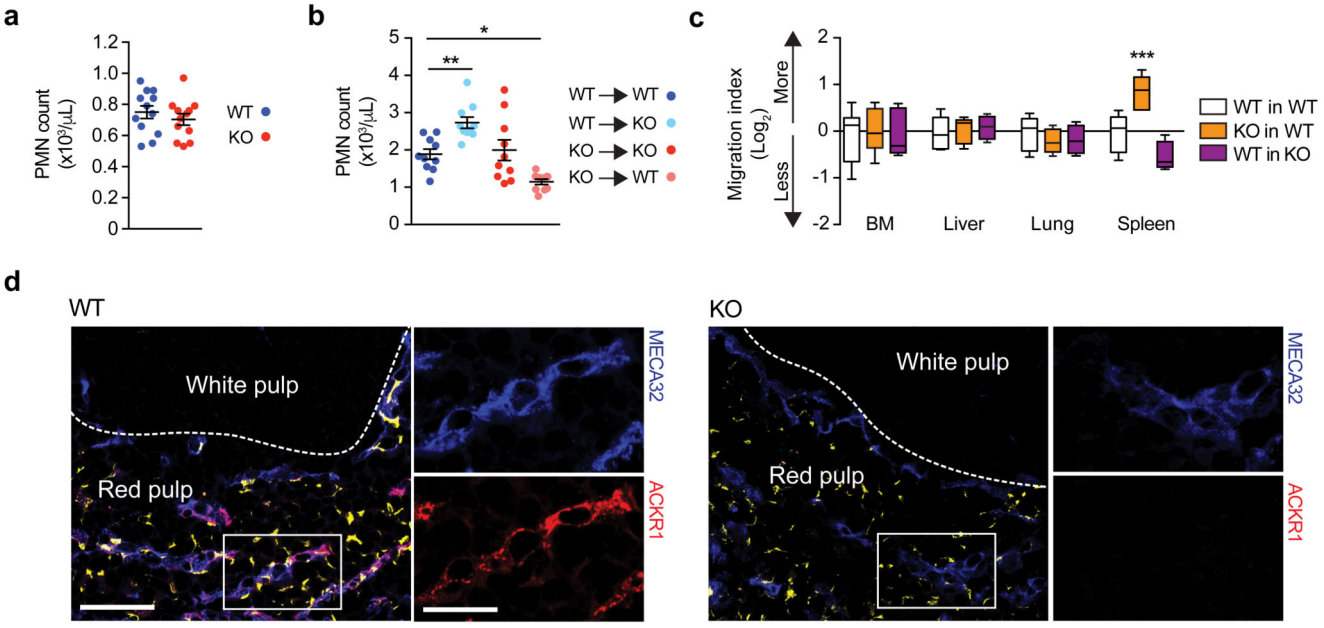

Fig. 8. Lack of ACKR1 on NECs and its expression on EC causes neutropenia.

(**a**) Blood neutrophil counts in wild-type (WT, blue) and ACKR1-deficient (KO, red) mice; n=12 from three independent experiments. (**b**) Blood neutrophil counts in reciprocal BM chimeric mice. n=10 from two independent experiments. WT reconstituted into WT (blue), WT reconstituted into KO (light blue), KO reconstituted into KO (red) and KO reconstituted into WT (pink). (**c**) Reciprocal homing of neutrophils of WT (purple) and KO (orange) mice into BM, liver, lungs and spleen of their respective KO and WT parabionts (n=5) compared to WT neutrophil homing into the organs of WT parabionts (white; n=8). (**d**) Representative immunofluorescence micrograph of WT mouse spleen stained with anti-ACKR1 (red) and anti-MECA32 (blue; ECs) and anti-Ter119 (yellow; erythrocytes). Insets show ACKR1 immunoreactivity in sinusoidal ECs. Scale bars, 50μm (main images) and 25μm (insets). All numeric data are Mean±SEM in dot-plots (**a,b**). For box plots (**c**), center lines represent the median; limits represent quartiles; whiskers represent minimum and maximum values. (**a**) two-tailed Student's t-test; (**b** and **c**) One-way ANOVA; *P < 0.05, **P < 0.01, ***P < 0.001.

Europe PMC Funders Author Manuscripts